

Magnetoelectric coupling effect of polarization regulation in $BiFeO_3/LaTiO_3$ heterostructures

Chao Jin(金超), Feng-Zhu Ren(任凤竹), Wei Sun(孙伟), Jing-Yu Li(李静玉), Bing Wang(王冰), and Qin-Fen Gu(顾勤奋)

Citation: Chin. Phys. B, 2021, 30 (**7**): 076105. DOI: 10.1088/1674-1056/abf924
Journal homepage: http://cpb.iphy.ac.cn; http://iopscience.iop.org/cpb

What follows is a list of articles you may be interested in

Prediction of scandium tetraboride from first-principles calculations: Crystal structures, phase stability, mechanical properties,and hardness

Bin-Hua Chu(初斌华)† and Yuan Zhao(赵元)
Chin. Phys. B, 2021, 30 (**7**): 076107. DOI: 10.1088/1674-1056/abe116

Ground-state structure and physical properties of YB_3 predicted from first-principles calculations

Bin-Hua Chu(初斌华), Yuan Zhao(赵元), and De-Hua Wang(王德华)
Chin. Phys. B, 2021, 30 (**4**): 046101. DOI: 10.1088/1674-1056/abcf94

Ab initio study on crystal structure and phase stability of ZrC_2 under high pressure

Yong-Liang Guo(郭永亮), Jun-Hong Wei(韦俊红), Xiao Liu(刘潇), Xue-Zhi Ke(柯学志), and Zhao-Yong Jiao(焦照勇)
Chin. Phys. B, 2021, 30 (**1**): 016101. DOI: 10.1088/1674-1056/abb3e7

Effects of Re, Ta, and W in [110] (001) dislocation core of γ/γ' interface to Ni-based superalloys: First-principles study

Chuanxi Zhu(朱传喜), Tao Yu(于涛)
Chin. Phys. B, 2020, 29 (**9**): 096101. DOI: 10.1088/1674-1056/abad26

Tunable electronic structures of germanane/antimonene van der Waals heterostructures using an external electric field and normal strain

Xing-Yi Tan(谭兴毅), Li-Li Liu(刘利利), Da-Hua Ren(任达华)
Chin. Phys. B, 2020, 29 (**7**): 076102. DOI: 10.1088/1674-1056/ab8a39

Magnetoelectric coupling effect of polarization regulation in $BiFeO_3/LaTiO_3$ heterostructures*

Chao Jin(金超)[1], Feng-Zhu Ren(任凤竹)[1,†], Wei Sun(孙伟)[1], Jing-Yu Li(李静玉)[1], Bing Wang(王冰)[1,‡], and Qin-Fen Gu(顾勤奋)[2,§]

[1] *Institute for Computational Materials Science, School of Physics and Electronics, International Joint Research Laboratory of New Energy Materials and Devices of Henan Province, Henan University, Kaifeng* 475004, *China*
[2] *Australian Synchrotron, ANSTO,* 800 *Blackburn Rd, Clayton, VIC,* 3168, *Australia*

(Received 23 February 2021; revised manuscript received 11 April 2021; accepted manuscript online 19 April 2021)

An effective regulation of the magnetism and interface of ferromagnetic materials is not only of great scientific significance, but also has an urgent need in modern industry. In this work, by using the first-principles calculations, we demonstrate an effective approach to achieve non-volatile electrical control of ferromagnets, which proves this idea in multiferroic heterostructures of ferromagnetic $LaTiO_3$ and ferroelectric $BiFeO_3$. The results show that the magnetic properties and two-dimensional electron gas concentrations of $LaTiO_3$ films can be controlled by changing the polarization directions of $BiFeO_3$. The destroyed symmetry being introduced by ferroelectric polarization of the system leads to the transfer and reconstruction of the Ti-3d electrons, which is the fundamental reason for the changing of magnetic properties. This multiferroic heterostructures will pave the way for non-volatile electrical control of ferromagnets and have potential applications.

Keywords: first-principles calculations, $BiFeO_3/LaTiO_3$ heterostructures, magnetoelectric coupling effect, polarization regulation

PACS: 61.50.Ah, 73.40.Lq, 75.70.Cn, 77.55.Nv **DOI:** 10.1088/1674-1056/abf924

1. Introduction

Traditional perovskite-type multiferroic compounds are a class of materials with general formula ABO_3, A-site deviates from the center of symmetry of the crystal to achieve spontaneous polarization and B-sites with unpaired electrons provides for spontaneous magnetic order, so they can accommodate various electronic and magnetic ground states.[1,2] These materials exhibit simultaneous ferromagnetism (FM) and ferroelectricity (FE), and the two ferric properties change with an external magnetic field and electric field. The novel magnetoelectric (ME) coupling effect enables multiferroics application in information storage, spintronic devices, magnetic sensors, and capacitor and inductor integrated devices.[3–8] However, single-phase multiferroics are quite rare at room temperature, because the ferromagnetic requires unpaired electrons in partially occupied d-orbitals or f-orbitals and ferroelectricity requires empty d-orbitals which is mutually exclusive in nature.[9–11] The ME coefficient is usually weak because there is associated with different ions, which is far from the application. Therefore, many researchers make a concerted effort to find the multiferroic composite materials and a study of the ME coefficient improvement at room temperature has become a research hotspot.

Heterogeneous multiferroics combining ferromagnetic and ferroelectric materials together can produce a strong magnetoelectric coupling effect.[9] Based on the heterostructures (HSs) of perovskite oxides, the FE and FM phases at the interface have been designed through advanced thin film material preparation technology to achieve the magnetoelectric coupling at the atomic scale.[12–14] Due to the strong correlation effect of d-orbital electrons,[15,16] the surface/interface of the HSs has lattice reorganization and electron reorganization which can produce a multi-degree-of-freedom interaction of "spin–orbit–charge–lattice",[1,6,17–19] such as, transition between metal and insulator, magnetism, two-dimensional electron gas (2DEG), *etc.*[17,20–22] 2DEG with high electron mobility has important applications in spintronic devices, and its existence strongly depends on the composition of the interface.[23] Once the material is synthesized, the characteristics of its interface are fixed, it is difficult to grow the system that can regulate 2DEG and magnetoelectric coupling.[24,25] Therefore, it is necessary to control the polarization direction of the ferroelectric material by applying electric field and then realize the control of properties at the interface.[2,26–28]

In the typical Mott–Hubbard insulator perovskite oxide $RTiO_3$ (R represents the trivalent rare-earth ions),[29–31]

*Project supported by the National Natural Science Foundation of China (Grant No. 12047517), the International Cooperation Project of Science and Technology of Henan Province, China (Grant No. 182102410096), the Natural Science Foundation of Henan Province, China (Grant No. 202300410069), and the China Postdoctoral Science Foundation (Grant Nos. 2020M682274 and 2020TQ0089).

†Corresponding author. E-mail: f.z.ren@henu.edu.cn
‡Corresponding author. E-mail: bwang@vip.henu.edu.cn
§Corresponding author. E-mail: qinfeng@ansto.gov.au

© 2021 Chinese Physical Society and IOP Publishing Ltd

$LaTiO_3$ (LTO) exhibits G-type antiferromagnetic (G-AFM),[32,33] and its band gap is small (~ 0.2 eV). At low carrier doping levels, LTO can easily become a metal, and thus lead to a metal-to-insulation transition occurs.[34,35] The 2DEG was found at the interface of two insulators $SrTiO_3/LaTiO_3$ and $SrTiO_3/LaAlO_3$.[36,37] In $LaAlO_3$/LTO HSs, the spin orbits in LTO could be effectively controlled by introducing $LaAlO_3$,[38,39] which is particularly important in magnetoelectric coupling devices. The $BiFeO_3$ (BFO) is the only room temperature single-phase multiferroic material with significant spontaneous polarization.[40,41] Compared with the rhombohedral phase BFO, the tetragonal phase BFO possesses larger spontaneous polarization and charge transfer excitation.[42–44] Due to the strong magnetoelectric coupling, the tetragonal BFO is often chosen as the substrate.[28] For instance, the study by Yin *et al.* showed that Fe_4N/BFO was anisotropy under the condition of adjustable electric field.[44,45] Yin *et al.* also found that the BFO/LTO superlattices had metal-insulation transition and 2DEG with different terminations.[19] It is well known, in artificially prepared superlattices, that the application of an external electric field can only affect the magnetic properties of the superlattice surface (it has little internal impact). However, the method of ferroelectric polarization control can effectively regulate the overall magnetic properties of the superlattice. Therefore, the BFO/LTO HSs are constructed, not only to introduce the surface/interface effect into the structure (we hope that the surface/interface effects can bring new characteristics to the HS), but also to control the spontaneous polarization of the material by applying electric field. This may achieve the purpose of controlling magnetism with polarization simultaneously. In addition, it is worthy of attention that the influence of the same interface and different polarization configurations on the electronic structure and magnetic properties for LTO thin films.

In our work, by using density functional theory (DFT) method, we mainly investigate the effect of the magnetic order and magnetic moment of the LTO film by changing the polarization direction of the BFO. The ideal interface without any defects and adsorption in the heterogeneous structure has been fully considered in our calculation model. In depth analysis shows that the difference of magnetic properties attributes to charge transfer from Ti-t_{2g} orbital to O-$p_{x,y}$ orbital and the electronic rearrangement inside Ti-t_{2g}. Besides, the 2DEG is also found in BFO/LTO HSs, and the inversion of the polarization direction gives rise to the change in the density of 2DEG. This work will be of great significance in the practical application of magnetoelectric storage materials.

2. Methods

Our first-principles calculations are carried out within the Perdew–Burke–Ernzerhof functional revised for solids (PBEsol).[46] The generalized gradient approximation (GGA) and projector-augmented wave (PAW) method are employed for the core-valance interaction and the exchange–correlations function,[5,47] which implemented in the Vienna *ab initio* simulation package (VASP).[46,48] The valance electrons configurations had been employed for Bi-$5d^{10}6s^26p^3$, Fe-$3d^74s^1$, O-$2s^22p^4$, La-$5s^25p^65d^16s^2$, and Ti-$3p^63d^24s^2$, respectively. The energy cut off for plane wave is chosen to be 500 eV and Γ-centered $7 \times 7 \times 1$ Monkhorst–Pack k-points meshes are performed in the Brillouin zones integration for the BFO/LTO HSs. Structural relaxation is performed until the Hellmann–Feynman force on each ion converged to be less than 0.03 eV/Å. The thickness of the vacuum layer is set to be 15 Å to avoid the interaction between periodic images of the z axis. In addition, to partially correct the Coulomb interaction on d orbitals, we adopt Hubbard $U_{\text{eff}} = 4$ eV of Fe 3d orbitals and $U_{\text{eff}} = 3$ eV for Ti 3d orbitals by the GGA + U method of Dudarev *et al.*'s approach.[10,19,28] Previous studies have shown that spin orbit coupling (SOC) has small influence on BFO and LTO.[19,28,49] Therefore, the SOC effect is not considered in this work.

The LTO thins grown along the [001] direction are widely studied.[19,32] Therefore, we constructed the BFO/LTO HSs along the [001] direction. While the lattice constants of BFO are matched on that of $SrTiO_3$ (STO) in the xy-plane, it can be simulated the growth of the multiferroics heterojunction on the STO substrate in experimentally.[19,28,49–51] And BFO can be grown on STO substrate to obtain tetragonal phase BFO. Thus, the BFO (001) slab is expanded into $\sqrt{2} \times \sqrt{2}$ as the substrate to support LTO (001) slab with the 1×1 unit cell. In the xy-plane, the lattice constants of BFO ($a = b = \sqrt{2}a\text{BFO} = 5.5217$ Å) are approach to the lattice constants of LTO ($a = 5.633$ Å, $b = 5.615$ Å). The lattice mismatch rates are only about 2.0% and 2.6% in the x and y directions, respectively. Objective to explore the magnetoelectric coupling effect of polarization regulation in the BFO/LTO HSs, we construct the BFO/LTO HSs model containing a minimum LTO unit of the intra-layer and inter-layer magnetic structure. Namely, every BFO/LTO HS model consists of 4 monolayers (ML) of the BFO part and 2 MLs of the LTO part. The bottom 2 MLs BFO ions are fixed to simulate a thin substrate, while the rest of the ion coordinates are completely relaxed, and finally make it reach a state of equilibrium. Four different interfaces (BiO/TiO_2, FeO_2/LaO, BiO/LaO, FeO_2/TiO_2) can be formed when constructing the BFO/LTO HS models. Among, the BiO/LaO and FeO_2/TiO_2 interfaces destroys the crystal symmetry of the perovskite structure, while the BiO/TiO_2 and FeO_2/LaO interfaces are better for crystal growth because they maintain perovskite structure. Moreover, previous calculations of the cohesive energy shown that the BiO/TiO_2 and FeO_2/LaO interfaces are more stable structures than the other two.[19] Therefore, only two interface BiO/TiO_2 (abbreviated

as BT-type) and the FeO_2/LaO (abbreviated as FL-type) HSs models are further considered in this work. Simultaneously, in order to investigate the effect of BFO polarization on the system, the net FE polarization of BFO along the $+z$ direction ($+P$) or the $-z$ direction ($-P$) is set. Four kinds of BFO/LTO models are set up here (Fig. 1).

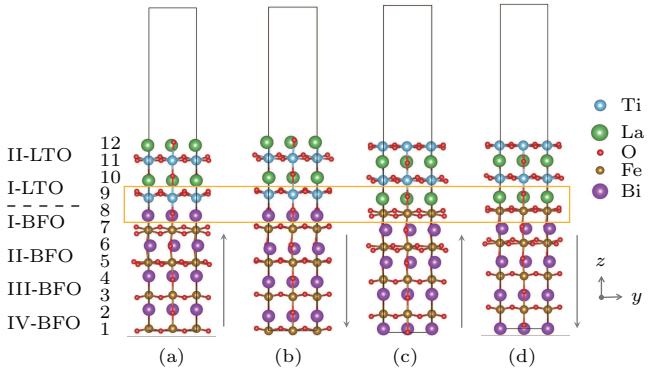


Fig. 1. (a)–(d) Side view along c axis of the BFO/LTO HSs for different terminals. Panels (a) and (b) are BiO/TiO_2 interface; (c) and (d) are FeO_2/LaO interface. The grey arrows represent the FE polarization of BFO, the up and down arrows mean respectively $+P$ and $-P$ states. The part enclosed by the yellow solid line is the interface part of the BFO/LTO HSs.

3. Results and discussion

In order to determine the stability of our established HSs models, the interfacial formation energy is calculated, which is defined as $E_{\text{form}} = (E_{\text{BFO/LTO}} - E_{\text{BFO}} - E_{\text{LTO}})/A$, where E_{form} is the formation energy of per unit area; $E_{\text{BFO/LTO}}$, E_{BFO}, and E_{LTO} are the total energy of the BFO/LTO HS, the BFO surface, and the LTO surface, respectively. A (30.264 Å^2) is the interface area of the BFO/LTO HS. The adsorption energies of the all BFO/LTO HSs models are listed in Table 1. The FL-type HSs have lower formation energies (E_{form}) than the BT-type HSs, indicating the FL-type HSs are more stable than the BT-type HSs. For the BT-type HSs, whether in the case of $+P$ or $-P$, the overall behaviour is a metallic state, meanwhile, the calculated magnetic order of BFO and LTO parts are all the G-AFM order and ferrimagnetic (FiM) order respectively (Table 1 and Table S1), which means that the physical properties of the BT-type HSs are not regulated by FE polarization. However, for the FL-type HSs, the magnetic order of LTO part changes FiM order from A-AFM when the polarization direction of BFO changes $-P$ from $+P$, which is also confirmed by the calculated exchange constants (Fig. S1 and Table S2). Thus, it is successfully realized the local FM order switched by the FE polarization at the I-LTO layer. More interestingly, changing the directions of polarization, the direction of the easy magnetization axis (EMA) also changes from [001] to [100]. By switching the different states of the easy magnetization axis, it is expected to be applied to logic devices. Based on the above analysis, it shows that the FL-type HSs are more energetically favourable and their magnetic order as well as magnetic anisotropy can be effectively controlled by FE polarization. Therefore, we only focus on the properties of the FL-type HSs in the below.

Table 1. Physical properties of the BFO/LTO HSs in the case of $+P$ and $-P$.

	BT-type		FL-type	
P_{BFO}	$+P$	$-P$	$+P$	$-P$
E_{form} (eV/Å^2)	−0.147	−0.403	−0.423	−0.464
Conductivity	metal	metal	metal	metal
2DEG	Yes	Yes	Yes	Yes
Magnetic order[a]	FiM	FiM	A-AFM	FiM
(LTO part)	↑↑	↑↑	↑↑	↑↑
	↑↓	↑↓	↓↓	↑↓
EMA	[100]	[100]	[001]	[100]

[a]Because the magnetic order of the BFO part always indicates G-AFM, the table only shows the magnetic order of the LTO part.

It is well known that the anion and cation displacement of the system reflects the change of its structure and interlayer electric dipole moment. The average displacements between anions and cations for the FL-type HSs are given in Fig. 2(a), the two vertical dotted portion represents the interface portion of the HSs. Firstly, we found that the central positions

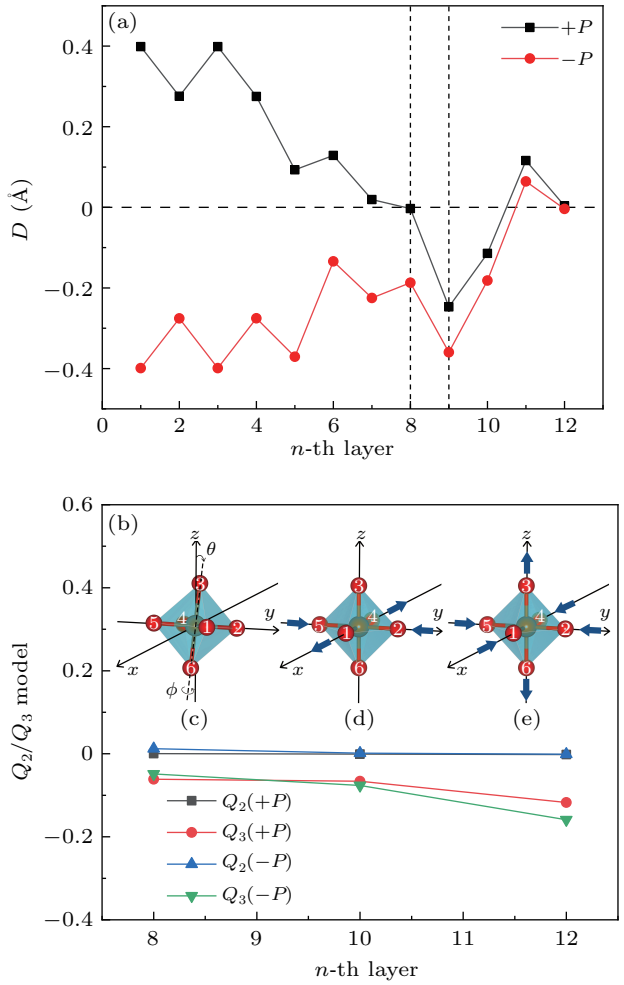


Fig. 2. (a) The average displacements between anions and cations (D) in the interlayer for FL-type HSs. (b) The deformation of the LTO part is described by the Jahn–Teller model of oxygen octahedra (Q_2 and Q_3). Panels (c), (d), (e) are the schematic diagrams of the tilting and rotation of the oxygen octahedron, Q_2 distortion, and Q_3 distortion, respectively.

of the anion could not overlap with that of the cation in each layer at the interface of the LTO parts under the BFO polarization, which indicates that the LTO parts are polarized and the oxygen octahedra of the LTO parts appear ferroelectric distortion and built-in electric field. Secondly, the change trend of the displacements between cations and anions under polarized states $+P$ is just the same as that of $-P$ in the LTO parts, which implies the LTO part is not sensitive to the BFO polarization direction. However, the average displacements between anions and cations near the interface in the case of $-P$ are larger than that of in the case of $+P$, owing that the direction of the built-in electric field due to ferroelectric distortion in the LTO part is the same as the direction of the polarized electric field of the BFO.[52] This qualitatively shows that the amount of charge transfer in the case of $-P$ is greater than that of in the case of $+P$. The transferred electrons caused by this kind of ferroelectric distortion ultimately lead to the emergence of 2DEG in the HSs.

The magnetic moments of the FL-type HSs and net magnetization of Fe and Ti atoms are further investigated as listed in Table 2. Combined with Tables 1 and 2, we find out that the BFO part always maintains the G-AFM order (in-plane antiparallel magnetic order and out-plane antiparallel magnetic order) for all the studied systems. This shows that the built-in electric field in the LTO part and interface reconstruction only affect the magnetic moment of the Fe atoms, but not alter the magnetic order of the BFO part. However, due to the reversal of polarization, the magnetic order of the LTO part changes from A-AFM to FiM, and the magnetic moment of Ti atoms decreases significantly. In addition, when LTO (space group *Pbnm*) and BFO (space group *P*4*mm*) form a heterostruction, BFO will suppress the $GdFeO_3$-type distortion of LTO. Moreover, in the process of structural relaxation, the symmetry of the system is broken due to the joint action of interface reconstruction, substrate fixation and FE polarization. This will cause the magnetic moments of the same layer of magnetic atoms to be slightly different, but this will not affect the qualitative analysis of magnetism. We also measured the average bond lengths of oxygen octahedra at the interface under the case of $+P$ and $-P$, which were 1.988 Å and 1.985 Å, respectively. The bond length under these two cases is slightly smaller than that of the bulk LTO value (2.002 Å), indicating that the polarization did not significantly influence the Ti–O bond length and the Ti–O bond length is not the main reason of the magnetic order change.

Table 2. Magnetic moments (Mag) and net magnetization (M) of Fe and Ti atoms in the FL-type HSs, as well as rotation angles (φ) and tilting angles (θ) for Jahn–Teller distortion of the LTO part in the case of $+P$ and $-P$.

	$+P$					$-P$			
Layer	Mag (μ_B)		φ (°)	θ (°)	Layer	Mag (μ_B)		φ (°)	θ (°)
II-LTO	0.599	0.601	−0.254	6.762	II-LTO	0.166	0.167	−0.961	5.813
I-LTO	−0.478	−0.497	9.326	8.534	I-LTO	−0.135	0.133	9.771	5.990
I-BFO	−4.497	4.475	–	–	I-BFO	−4.439	4.438	–	–
II-BFO	4.508	−4.508	–	–	II-BFO	4.436	−4.436	–	–
M	–	0.197	–	–	M	–	0.145	–	–

In order to explore the influence of the oxygen octahedra in the LTO part on the magnetic order, we further investigated the Jahn–Teller (JT) distortion mode Q_2/Q_3 (breaking the symmetry, thereby splitting the t_{2g} orbit).[53] The schematic diagrams of the tilting and rotation of the oxygen octahedron, Q_2 distortion, and Q_3 distortion are shown in Figs. 2(b)–2(e). The JT distortion mainly includes Q_2 and Q_3 modes.[54] The changes of the two modes are expressed as: $Q_2 = (1/\sqrt{2})(X_1 - X_4 - Y_2 + Y_5)$ and $Q_3 = (1/\sqrt{6})(2Z_3 - 2Z_6 - X_1 + X_4 - Y_2 + Y_5)$, where X, Y, and Z are expressed as the coordinates of O atoms around the Ti atom, and the subscripts represent different O atoms around the oxygen octahedra. As shown in Fig. 2(b), the Q_3 distortion of the oxygen octahedra is slightly more obvious than the Q_2 distortion. However, whether under the case of $+P$ or $-P$, there is no significant difference in the effects of polarization on Q_2 and Q_3 distortions in general. Whereas, Q_3 is always distorted to a negative value whether $+P$ or $-P$, indicating that the oxygen octahedra are compressed along the z-axis direction, which inhibits the electron occupation of Ti-d_{yz}/d_{zx} orbit and makes electrons more inclined to occupy Ti-d_{xy} orbit. In addition to the JT distortion of the oxygen octahedra mentioned above, there are two important physical quantities that must be considered, namely the rotation angle (φ) and the tilt angle (θ) of the oxygen octahedra,[2] which affect the properties of the perovskite HSs to some extent. As can be seen from φ and θ in Table 2, the rotation angle and tilting angle change consistently when the polarization direction inverse. According to the above analysis of the rotation angles, tilting angles, and Q_2/Q_3 distortion, it can be concluded that the polarization has little effect on the oxygen octahedra rotation and JT distortion in this system, which are not also the reason for magnetic order changes. In order to discuss whether the magnetic change of the system is caused by d-electron transfer, next the electronic structure of HSs was analysed.

In order to qualitatively explain the physical mechanism of magnetic regulation, we analysed the density of states (DOS) of the FL-type HSs (Fig. 3). No matter in the case

of $+P$ or $-P$, the total density of state (TDOS) at the Fermi level is not zero, indicating that HSs exhibit the characteristics of metal. As can be seen from the layered density of state (LDOS), the DOS at Fermi level is attributed dominantly by the Ti-3d states. The BFO part is insulated, while the LTO part is conductive, indicating that the electron can only move in the *xy*-plane to form a 2DEG. The concentration of 2DEG in the case of $+P$ is higher than that of in the $-P$ case, which further reflects that the conductivity of the HSs in the case $+P$ is stronger than that of in the case $-P$. Simultaneously, with the reversal of polarization, the Ti-3d state moves to the high energy region and the occupancy of Ti-3d near the Fermi level is getting smaller gradually, the interface I-LTO layer changes from metal to insulating state. In addition, in the case of $+P$, the 2DEG exhibits ferromagnetism in I-LTO and II-LTO parts respectively owing to the dominance of same spin polarized (spin-up or spin-down) states, while the whole system exhibits A-AFM.

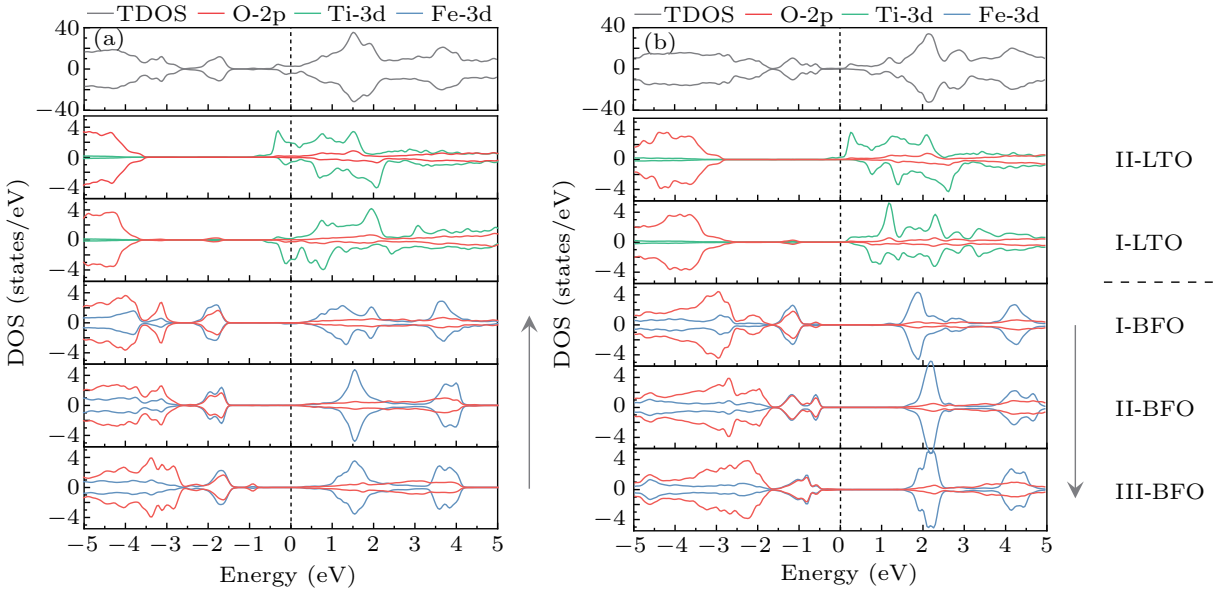


Fig. 3. For FL-type HS, panels (a) and (b) are expressed as TDOS and LDOS in the case of $+P$ and $-P$, respectively. The solid grey line indicates TDOS; The solid blue line represents the Fe-3d states. The solid green line represents the Ti-3d states. The solid red line represents the O-2p states. The black dotted line represents the Fermi level. The up and down grey arrows represent $+P$ and $-P$ states, respectively.

Table 3. The average transferred electron numbers for the Ti-t_{2g} (d_{xy}, d_{yz}, d_{zx}) orbitals in the FL-type HSs relative to that of the bulk LTO under the $+P$ and $-P$ cases.

	d_{xy}	d_{yz}	d_{zx}	Total
$+P$	−0.214	−0.159	0.282	−0.091
$-P$	−0.426	−0.540	−0.096	−1.062

For perovskite transition metal oxides, the arrangement of 3d orbitals usually determines its electronic structure and physical properties. Due to the effect of the octahedral symmetry field, the 3d orbitals will split into t_{2g} and e_g. To better elucidate the microscopic mechanism of the change of magnetic order and magnetic moment, we perform an elaborate DOS analysis of Ti-3d and O-2p in LTO parts, as shown in Fig. 4. It can be clearly seen the states at the Fermi level and the magnetic moments of the LTO parts are substantially ascribed to the partially occupied Ti-t_{2g} orbital. When the polarization is reversed, there is a strong hybrid between the Ti-t_{2g} orbital and the O-$p_{x,y}$ orbital, so that the electrons in the t_{2g} orbital move toward O-$p_{x,y}$ orbit transfer and the occupation of electrons in the Ti-t_{2g} orbital at the Fermi level decreases. Therefore, the magnetic moment of Ti atoms at the II-LTO layer changes from 0.6 μ_B to 0.166 μ_B, and the magnetic moment of Ti atom at the I-LTO layer changes from 0.487 μ_B to 0.134 μ_B. It can be seen from Figs. 4(c) and 4(d) that, in the case of $+P$ and $-P$, the shape and trend of the PDOS are significantly different for the I-LTO layer.Therefore, we further draw PDOS of d_{xy}, d_{yz}, and d_{zx} orbits for the I-LTO layer Ti atoms as shown in Figs. 4(e) and 4(f). We can see that the energy of the d_{xy} orbit is lower than the d_{zx} and d_{yz} orbits, which is consistent with the tendency of electrons to occupy d_{xy} orbitals due to the Q_3 distortion induced compression of oxygen octahedron along z direction. We also integrate the state density of the d_{xy}, d_{yz}, and d_{zx} orbitals to obtain the corresponding transferred electron numbers for Ti-d_{xy}, Ti-d_{yz}, and Ti-d_{zx} orbits in the FL-type HSs relative to that of in the bulk LTO, as presented in Table 3. When the FE polarization is $+P$, the Ti-$d_{xy/yz}$ orbital loses electrons relative to the bulk LTO, and the d_{zx} orbital gains electrons, which is likely to change the magnetic order of the LTO part from G-AFM to A-AFM. When the FE polarization is changed to $-P$, the main $d_{xy/yz}$ orbital loses electrons, and the overall Ti-t_{2g} orbital loses electrons more. This leads to the emergence of net magnetic moment in the system, which in turn changes the magnetic order of the LTO part from G-AFM to FiM. As simple summary of

the above, FL-type HSs exhibits different properties from the bulk LTO. The FE polarization state of the substrate changes the magnetism of the LTO part at the interface. Due to the combined effect of the electron transfer between the Ti-3d and O-2p orbitals and the electron transfer inside the Ti-t_{2g} orbital, the magnetic order of the system changes.

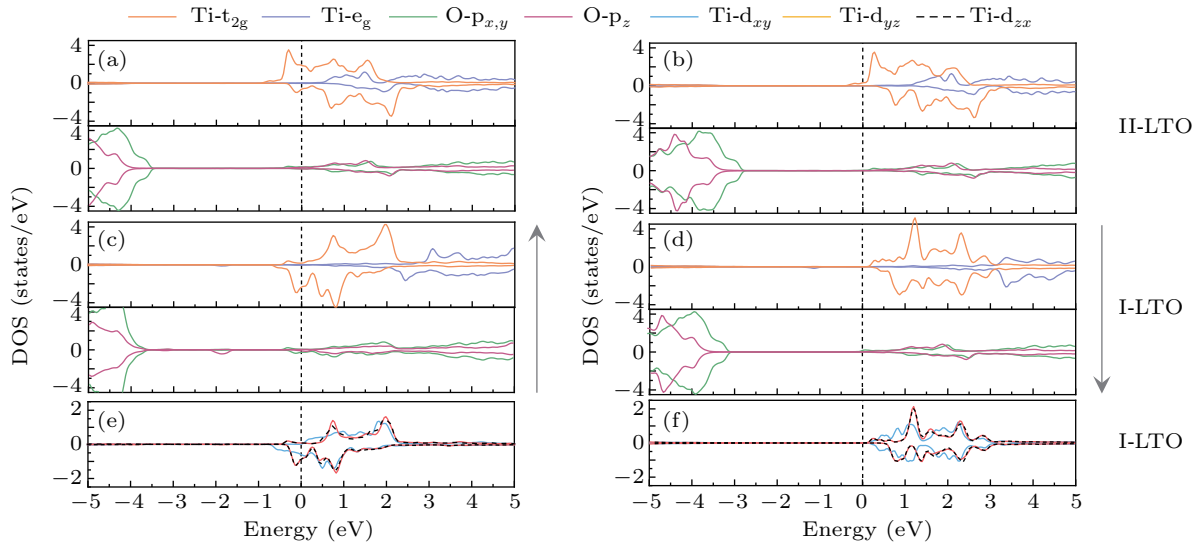


Fig. 4. The projected-DOS (PDOS) are shown for the FL-type HSs in the $+P$ and $-P$ cases. Where panels (a) and (b) are the PDOS of the II-LTO layer; panels (c) and (d) are the PDOS of the I-LTO layer; panels (e) and (f) are the PDOS of Ti-d_{xy}, Ti-d_{yz}, and Ti-d_{zx} orbitals for the I-LTO layer. The up and down grey arrows represent $+P$ and $-P$ states, respectively.

4. Conclusion

In summary, we calculated the magnetic and electronic structure of the multiferroic BFO/LTO HSs. This performance can be adjusted by changing the FE polarization direction in the BFO/LTO HSs. We found that for the BT-type heterostructure, the polarization reversal has no effect on the magnetic and electronic structure. For the FL-type heterostructure, in the case of $+P$, the magnetic order of the LTO part is A-AFM, and the heterojunction as a whole is metallic. The appearance of 2DEG can be clearly observed at the interface, indicating that it has strong conductivity. In the case of $-P$, the LTO part is FiM ordered and shows metallicity and appears 2DEG as well, but the concentration of 2DEG is lower than that of in the case of $+P$, which means that the conductivity is reduced. According to the analysis of crystal structure and electronic structure, the change of the magnetic order is mainly caused by the charge transfer inside Ti-t_{2g} orbitals. Our work provides theoretical guidance for the control of physical properties through the re-orientation of FE polarization. This method of using polarization reversal to control conductivity and magnetic properties can be applied in future electronic devices.

References

[1] Cossu F, Singh N and Schwingenschloegl U 2013 *Appl. Phys. Lett.* **102** 042401
[2] He J, Borisevich A, Kalinin S V, Pennycook S J and Pantelides S T 2010 *Phys. Rev. Lett.* **105** 227203
[3] Wang B, Zhang X W, Zhang Y H, Yuan S Y, Guo Y L, Dong S and Wang J L 2020 *Mater. Horiz.* **7** 1623
[4] Wang B, Zhang Y H, Ma L, Wu Q S, Guo Y L, Zhang X W and Wang J L 2019 *Nanoscale* **11** 4204
[5] Hou F, Cai T Y, Ju S and Shen M R 2012 *Acs Nano* **6** 8552
[6] Cao D, Cai M Q, Hu W Y, Peng J, Zheng Y and Huang H T 2011 *Appl. Phys. Lett.* **98** 031910
[7] Cheng J, Nazir S and Yang K 2016 *ACS Appl. Mater. Inter.* **8** 31959
[8] Wang B, Wu Q S, Zhang Y H, Guo Y L, Zhang X W, Zhou Q H, Dong S and Wang J L 2018 *Nanoscale Horiz.* **3** 551
[9] Chen D, Zhang G B, Cheng Z X, Dong S and Wang YX 2019 *IUCrJ* **6** 189
[10] Chen L, Xu C S, Tian H, Xiang H J, Iniguez J, Yang Y R and Bellaiche L 2019 *Phys. Rev. Lett.* **122** 247701
[11] Dong S, Xiang H and Dagotto E 2019 *Natl. Sci. Rev.* **6** 629
[12] Wen F D, Cao Y W, Liu X R, Pal B, Middey S, Kareev M and Chakhalian J 2018 *Appl. Phys. Lett.* **112** 122405
[13] An M, Weng Y K, Zhang H M, Zhang J J, Zhang Y and Dong S 2017 *Phys. Rev. B* **96** 235112
[14] Yao F, Zhang L F, Meng J L, Liu X J, Zhang X, Zhang WW, Meng J and Zhang H J 2018 *J. Appl. Phys.* **123** 115304
[15] Lee M, Choi H and Chung Y C 2013 *J. Appl. Phys.* **113** 425
[16] Mellan T A, Corà F, Grau-Crespo R and Ismail-Beigi S 2015 *Phys. Rev. B* **92** 085151
[17] Tseng A, Pham A, Smith S C and Li S 2016 *J. Appl. Phys.* **119** 075301
[18] Weng Y K, Zhang J J, Gao B and Dong S 2017 *Phys. Rev. B* **95** 155117
[19] Yin L, Mi W B and Wang X C 2015 *J. Mater. Chem. C* **3** 11066
[20] Dong S and Dagotto E 2013 *Phys. Rev. B* **88** 140404
[21] Li Y, Sun X Y, Xu C Y, Cao J, Sun Z Y and Zhen L 2018 *Nanoscale* **10** 23080
[22] Xue Y B, Zhao J Z, Shan Y Y and Xu H 2018 *Physica E* **98** 120
[23] Wei L Y, Lian C and Meng S 2017 *Phys. Rev. B* **95** 184102
[24] Karthikeyan R and Niranjan M K 2019 *J. Magn. Magn. Mater.* **469** 138
[25] Nanda B R K and Satpathy S 2008 *Phys. Rev. B* **78** 054427
[26] Dash S, Choudhary R N P, Das P R and Kumar A 2014 *Appl. Phys. A* **118** 1023
[27] Hou Y S, Xiang H J and Gong X G 2014 *Phys. Rev. B* **89** 064415
[28] Sun W, Wang W X and Chen D 2019 *J. Phys. Chem. C* **123** 16393
[29] Larson P, Popović Z C and Satpathy S 2008 *Phys. Rev. B* **77** 245122
[30] Okatov S, Poteryaev A and Lichtenstein A 2005 *Europhys. Lett.* **70** 499
[31] Veit M J, Chan M K Ramshaw B J 2019 *Phys. Rev. B* **99** 115126
[32] Weng Y K, Huang X and Tang Y K 2014 *J. Appl. Phys.* **115** 17E108
[33] Mochizuki M Imada M 2004 *New J. Phys.* **6** 154
[34] Lichtenberg F, Widmer D, Bednorz J G, Williams T and Reller A 1991 *Z. Phys. B* **82** 211
[35] Tokura Y, Taguchi Y, Okada Y, Fujishima Y and Iye Y 1993 *Phys. Rev. Lett.* **70** 2126
[36] Sheets W C, Boullay P and Lüders U U 2009 *Thin Solid Films* **517** 5130

[37] Ohtomo A and Hwang H Y 2004 *Nature* **427** 423
[38] Kan E J 2013 *Adv. Mater.* **771** 7
[39] Lee A T and Han M J 2014 *Phys. Rev. B* **89** 115108
[40] Feng N, Mi W B and Wang X C 2015 *ACS Appl. Mater. Inter.* **7** 10612
[41] Wang H, Zheng Y and Cai M Q 2009 *Solid State Commun.* **149** 641
[42] Lu Z X, Li P L and Wan J G 2017 *ACS Appl. Mater. Inter.* **9** 27284
[43] Bai X F, Wei J and Tian B B 2016 *J. Phys. Chem. C* **120** 3595
[44] Yin L, Wang X and Mi W 2016 *Phys. Rev. Appl.* **6** 064022
[45] Yin L, Wang X and Mi W 2017 *ACS Appl. Mater. Inter.* **9** 15887
[46] Perdew J P, Ruzsinszky A and Csonka G I 2008 *Phys. Rev. Lett.* **102** 039902
[47] Blochl P E 1994 *Phys. Rev. B* **50** 17953
[48] Kresse G and Furthmüller J 1993 *Phys. Rev. B* **47** 558
[49] Sun W, Wang W X and Chen D 2019 *J. Mater. Chem. C* **7** 463
[50] Zhang H M, Weng Y K and Yao X Y 2015 *Phys. Rev. B* **91** 195145
[51] Zhou P X, Liu H M and Yan Z B 2014 *J. Appl. Phys.* **115** 423
[52] Wang F, Li J and Du Y 2015 *Appl. Surf. Sci.* **355** 1316
[53] Dagotto E, Hotta T and Moreo A 2001 *Phys. Rep.* **344** 1
[54] Hashimoto T, Ishibashi S and Terakura K 2010 *Phys. Rev. B* **82** 045124